Evidence of molecular hydrogen trapped in two-dimensional layered titanium carbide-based MXene

Naresh C. Osti,[1,*] Michael Naguib,[2] Madhusudan Tyagi,[3,4] Yury Gogotsi,[5] Alexander I. Kolesnikov,[1] and Eugene Mamontov[1]

[1]*Chemical and Engineering Materials Division, Oak Ridge National Laboratory, Oak Ridge, Tennessee 37831, USA*

[2]*Materials Science and Technology Division, Oak Ridge National Laboratory, Oak Ridge, Tennessee 37831, USA*

[3]*NIST Center for Neutron Research, National Institute of Standards and Technology, Gaithersburg, Maryland 20899, USA*

[4]*Department of Materials Science, University of Maryland, College Park, Maryland 20742, USA*

[5]*Department of Materials Science and Engineering, A.J. Drexel Nanomaterials Institute, Drexel University, Philadelphia, Pennsylvania 19104, USA*

(Received 20 April 2017; revised manuscript received 5 June 2017; published 17 July 2017)

Two-dimensional transition metal carbides and nitrides (MXenes) are one of the largest and fastest growing families of materials. The presence of molecular hydrogen at ambient conditions in a MXene ($Ti_3C_2T_x$, where T_x represents a surface terminating species, including O, OH, and F) material is revealed here by inelastic and elastic neutron scatterings. The inelastic neutron-scattering spectrum measured at 5 K shows a peak at 14.6 meV, presenting a clear indication of the presence of parahydrogen in the MXene synthesized using 48% hydrofluoric acid and annealed at 110 °C in vacuum prior to the measurement. An increase in the measurement temperature gradually reduces the peak intensity and increases the peak width due to the mobility of the molecular hydrogen in confinement. The presence of molecular hydrogen is confirmed further from the observed elastic intensity drop in a fixed energy-window scan of elastic intensity measurements in the temperature range of 10–35 K. Using milder etching conditions, ion intercalation, or an increase in the annealing temperature all result in the absence of the trapped hydrogen molecules in MXene. The results of this paper can guide the development of MXene materials with desired properties and improve our understanding of the behavior of MXenes in applications ranging from supercapacitors to hydrogen evolution reaction catalysis and hydrogen storage.

DOI: 10.1103/PhysRevMaterials.1.024004

I. INTRODUCTION

Two-dimensional (2D) transition metal carbides and nitrides (MXenes) are a large family of 2D materials [1,2]. They have shown a potential to improve the efficiency of electrochemical energy storage devices when used as electrode materials [3,4]. Furthermore, MXenes also have shown their potential for water purification and sensor applications [5]. MXenes are represented by the general formula of $M_{n+1}X_nT_x$. They are produced from parent $M_{n+1}AX_n$ (MAX) phases by selective etching of the A layers composed of Al using hydrofluoric (HF) acid [6]. M and X layers, which are composed of early transition metals, and C and/or N, respectively, remain unaffected by acid treatment. Structure studies [7,8] using experiments and multimodal labeling have shown -O, -F, or -OH as surface groups (T_x) in MXene layers (n = 1–3). Two-dimensional morphology of MXenes, similar to clays, allows intercalation of different chemical species (organic, inorganic molecules, and metal ions) [9–11]. Traditionally, intercalation of clay minerals is performed in order to modify their properties for desired applications [12]. For example, intercalation of clay with silica results in a hybrid material having a high surface area and properties suitable for hydrogen adsorption [13]. Intercalated clays and clay-supported materials exhibit enhanced performance for hydrogen storage [14]. Similar to clays, numerous studies of pristine and intercalated MXenes have shown changes in the structure and electrochemical behaviors after intercalation [10,11,15,16]. Furthermore, a theoretical study suggested the possibility of using MXenes for hydrogen storage application [17], and MXenes also have been explored for hydrogen evolution in hydrogen evolution reaction catalysis [18] and in electrochemical testing of $Ti_3C_2T_x$ supercapacitor electrodes [19], but in this paper, we detect the presence of molecular hydrogen in MXenes.

Here, using inelastic and elastic neutron-scattering techniques, we report the presence of molecular hydrogen in a pristine $Ti_3C_2T_x$, a MXene synthesized using 48% HF to etch Al from Ti_3AlC_2. Inelastic neutron scattering (INS) and quasielastic neutron scattering have been powerful tools for studying the structure and dynamics of hydrogen-bearing species, such as hydrogen [20–22] and water [23–25] in confinement because of the much larger neutron-scattering cross section of hydrogen atoms [$\sigma_s(H) = 82.02$ b] compared to other atoms (e.g., σ_s is 5.551, 4.232, 4.018, 1.503, and 4.35 b for C, O, F, Al, and Ti, respectively). Furthermore, we show that changes in the synthesis procedure, intercalation, or increases in annealing temperature eliminate the molecular hydrogen trapped in the MXene. Our findings open an avenue for the possible use of MXenes as hydrogen storage materials.

II. EXPERIMENT

A. Sample preparation

1. Synthesis of MXene using 48% *and* 10% *HF*

The powder of the parent MAX phase (Ti_3AlC_2, the synthesis procedure is described elsewhere [1]) of <45-μm particle sizes was immersed in aqueous HF (Macron Fine Chemicals—Avantor Performance Materials, Center Valley, PA) solutions with concentration of 48% (as the received acid) or 10% [diluted using de-ionized (DI) water]. The

*Author to whom correspondence should be addressed: ostinc@ornl.gov

mixture was stirred for 24 h at room temperature (RT). The chemical reaction of etching Ti_3AlC_2 in HF involves hydrogen evolution: $Ti_3AlC_2 + 3HF = Ti_3C_2 + AlF_3 + 3/2\,H_2$. This hydrogen can be trapped between MXene layers. $Ti_3C_2T_x$ powder was obtained after several rounds of washing with DI water until the pH > 4, followed by vacuum filtration, air drying at RT, and finally annealing at 110 °C in vacuum. K^+-intercalated MXene was produced by mixing 1 g of 48% HF etched $Ti_3C_2T_x$ powder with 10 ml of $2M$ potassium hydroxide (KOH) aqueous solution. The mixture was stirred for an hour at RT and centrifuged. The sediment again was mixed with $2M$ KOH solution in the same ratio as before and stirred for 1 h at RT again. Afterward, the mixture was centrifuged, and the liquid was decanted. The settled powders were transferred using fresh DI water from the centrifuging vial to a vacuum-assisted filtration apparatus. The drying process was similar to what was described above.

2. *Synthesis of MXenes using a mixture of* 10% *HF and LiCl*

Ti_3AlC_2 powder was etched using a mixture of 10% HF and LiCl as an etchant at RT. The use of such an etchant produces MXenes with inherent intercalated metal ions that would allow fine-tuning of the MXenes' structure to optimize their properties for their technological applications [26]. The concentration of LiCl was maintained at a 5:1 molar ratio with Ti_3AlC_2 and processed as described previously. However, the product was prewashed with $6M$ HCl three times right after etching before drying the sediment in order to remove traces of precipitated salts and exchange intercalated Li with protons, i.e., form $Ti_3C_2T_x$-H. Then the powders were washed using DI water until the pH reached the values of more than 4 and dried as described above for the other samples. MXene samples were vacuum annealed at either 110 °C or 150 °C as needed. Samples were loaded inside an argon-filled glovebox in flat aluminum containers, which were sealed with indium for neutron-scattering measurements.

B. Neutron scattering

Inelastic neutron-scattering experiments were performed using the Fine Resolution Fermi Chopper Spectrometer (SEQUOIA) [27,28] at the Spallation Neutron Source at Oak Ridge National Laboratory. Data were collected with incident neutron energies (E_i) of 30 and 50 meV. The obtained time-of-flight data were transferred to the dynamical structure factor $S(Q,E)$, where E is the neutron energy transfer and Q is the momentum transfer, or to the generalized vibrational density of states (GVDOS) $G(E)$ by using MANTIDPLOT [29] and DAVE [30] software packages. The background spectra from the empty container were measured under similar conditions and subtracted from the sample data.

Elastic neutron-scattering measurements were carried out at the National Institute of Standards and Technology (NIST) Center for Neutron Research using a high-flux backscattering spectrometer (HFBS) [31]. The HFBS covers a dynamic range of $\pm 15.56\,\mu$eV with an energy resolution of $0.8\,\mu$eV [full width at half maximum (FWHM)]. The HFBS instrument was operated at the fixed-window mode by stopping the Doppler-drive motion of the neutron monochromator. Elastic intensity as a function of temperature was recorded from 5 to 300 K at a heating rate of 2 K/min. The elastic intensity for a sample was obtained by summing the intensity over all 16 detectors. The desired temperatures of measurements for both instruments (5–50 K for SEQUOIA and 5–300 K for HFBS) were reached using the bottom and top loading closed cycle helium refrigerators, respectively.

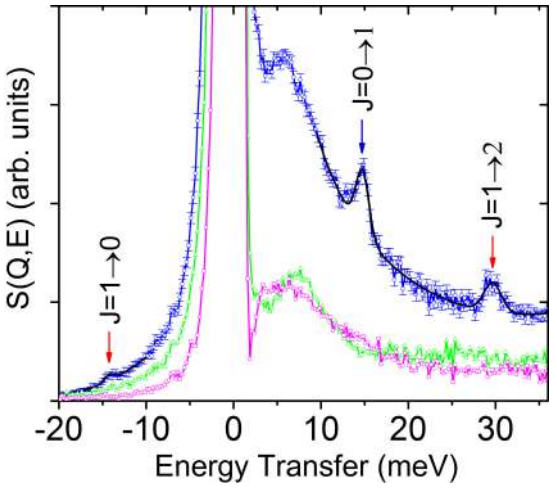

FIG. 1. Inelastic neutron-scattering spectrum of MXene synthesized using 48% HF ($Ti_3C_2T_x$) and annealed at 110 °C measured for 2 h at the SEQUOIA spectrometer with $E_i = 50$ meV immediately after cooling the sample to $T = 8$ K (blue circles: error bars represent one standard deviation). For comparison, the INS spectra also are shown for MXenes synthesized using 48% HF ($Ti_3C_2T_x$) and annealed at 150 °C (pink squares), and synthesized using 10% HF ($Ti_3C_2T_x$-H) and annealed at 110 °C (green triangles) where the data were collected after the samples were cooled to $T = 8$ K for 7 and 4 h, respectively.

III. RESULTS AND DISCUSSION

A MXene sample (hereafter, $Ti_3C_2T_x$) was synthesized using 48% HF and annealed at 110 °C in vacuum. Figure 1 shows the INS spectra of MXene samples measured with $E_i = 50$ meV immediately after cooling the sample from room temperature to $T = 8$ K. It is known that water [24] and hydroxyl groups [7] are the hydrogen-bearing species that are present in MXene. Translational modes of confined water could be visible in the INS spectra at low energies where a peak around 5–10 meV for amorphous ice and bulklike confined water also was observed [32–35]. The presence of hydroxyl groups gives separate wagging mode peaks arising from O-H bond oscillations at higher energies (between 50 and 160 meV) [35]. Therefore, the peaks detected at the energy of about 6 meV should mostly be related to the translational vibrations of water confined in all the MXene samples studied [36]. In addition to these peaks and the elastic peak (around $E = 0$ meV), there are three more peaks in the INS spectrum of $Ti_3C_2T_x$ annealed at 110 °C, which are observed at energies of -14.2, 14.7, and 29.7 meV. For the material in the equilibrium state, the intensity of the vibrational peaks (of energy E_v) in the INS spectrum is proportional to $n(E_v,T)$ and $n(E_v,T)+1$, respectively, for neutron energy gain and loss sides of the spectrum, where $n(E_v,T) = [\exp(E_v/k_BT) - 1]^{-1}$ is the

population Bose factor. For $E_v = 14.2$ meV at $T = 8$ K the Bose factor is on the order of 10^{-9}, so the observation of the peak at -14.2 meV in the INS spectrum indicates that this peak corresponds to neutron scattering on nonequilibrium states.

The peaks at 14.7 and 29.7 meV in $Ti_3C_2T_x$, which are absent in $Ti_3C_2T_x$-H and $Ti_3C_2T_x$ annealed at 150 °C, are characteristic features due to transitions between the para- and the orthostates in molecular hydrogen [37]. The energies of the quantum rotational levels of H_2 can be given by $E_J = BJ(J+1)$, where B is the rotational constant of the molecule ($B = 7.35$ meV for free H_2) and J is the rotational quantum number. The peak at 14.7 meV exactly corresponds to the para- ($J = 0$) to ortho- ($J = 1$) transition in molecular hydrogen, and the peak at 29.7 meV should be due to the ortho- ($J = 1$) to para- ($J = 2$) transition (it is 29.4 meV for free H_2). At room temperature, molecular hydrogen contains 75% of ortho- and 25% of parahydrogen. As the temperature is decreased, the concentration of parahydrogen increases, and at low temperatures (<10 K) the equilibrium state consists almost entirely of parahydrogen. It also is known that the ortho- to para-state conversion rate of pure molecular hydrogen at low temperatures is rather small. At ambient pressure, the conversion in the solid hydrogen takes weeks to equilibrate (see, e.g., Ref. [37]). Therefore, we conclude that the $Ti_3C_2T_x$ sample we used in the first measurement (immediately after cooling it from room temperature to 8 K) contained a significant amount of orthohydrogen, and the peaks observed at -14.2 and 29.7 meV correspond to $J = 1$ to $J = 0$ and $J = 1$ to $J = 2$ transitions, respectively (from ortho- to parahydrogen). To understand the state of H_2 molecules in $Ti_3C_2T_x$ (whether it is bulklike H_2 located in large cavities or pores or somewhat isolated H_2 molecules located in small structure openings), we measured the temperature dependence of the para- to ortho-H_2 transition peak ($J = 0$ to $J = 1$ at $E = 14.7$ meV) in the INS spectra collected with $E_i = 30$ meV. In the case of bulk hydrogen [38], the para- to orthopeak disappears at temperatures above 14 K (hydrogen melting temperature), whereas for confined molecular hydrogen, the peak can be observed up to much higher temperatures (~80 K) [20,39]. For equilibration purposes, the $Ti_3C_2T_x$ sample was cooled to 70 K, then slowly cooled to 5 K over 20 h, and exposed at $T = 5$ K for 29 h before the measurements. Then 1-h-long INS measurements were performed from 5 to 32 K with 3-K temperature increments. To check if the confined hydrogen was in the equilibrium state, the sample again was cooled to $T = 5$ K, and we repeated the measurements at the same temperatures. Importantly, we did not observe the peak at -14.2 meV in these measurements, which indicates the complete transformation of orthohydrogen to a parastate at low temperatures. This can be attributed to the electronic and nuclear interactions of orthohydrogen with the $Ti_3C_2T_x$ confinement that results in a transition of the quantum rotational state [40].

Figure 2 shows the INS spectra of trapped molecular parahydrogen at different temperatures from 5 to 32 K summed over the Q range of 0.4–3.4 Å^{-1}. The inset displays a (Q,E) contour plot of the $S(Q,E)$ spectrum measured at $T = 5$ K where the intense peak centered at ~14.6 meV due to the para-ortho-transition clearly is seen within the Q range covered by the spectrometer. It is known that confinement could cause changes in the peak position [41–43], depending on strength

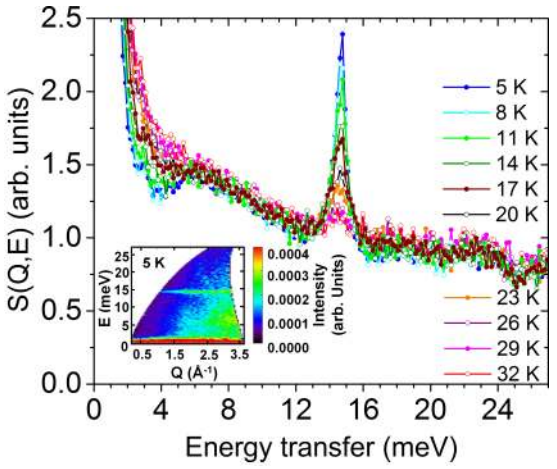

FIG. 2. Inelastic neutron-scattering spectra of MXene (synthesized using 48% HF and annealed at 110 °C in vacuum) measured with $E_i = 30$ meV at different temperatures. The inset shows a (Q,E) contour plot of the $S(Q,E)$ spectrum measured at $T = 5$ K.

of the H_2 interaction with the confining environment; therefore the observed very small shift (compared to free H_2) indicates that this interaction is weak and hydrogen has a significant freedom for rotation [20,42] similar to what was reported for hydrogen absorbed in single walled carbon nanotubes. Comparing the INS spectrum of $Ti_3C_2T_x$ MXene synthesized using 48% HF to the spectrum of the sample with the calibrated amount of H_2, we estimate that the amount of molecular hydrogen trapped in the MXene is about 0.3 wt % (which is about 25% of H_2 molecules per MXene formula unit Ti_3C_2).

The position of the para- to ortho-H_2 transition peak (at 14.6 meV) is not changing with temperature variation (Fig. 2), however, the intensity of the peak progressively decreases as temperature increases from 5 to 32 K, and finally it almost disappears. If the hydrogen exists as large clusters (the bulklike state), it should melt (at ~14 K) on increasing the temperature, resulting in a significant increase in the mean-squared displacement and causing an abrupt change in the peak intensity [44], which we do not observe in the experiment. Thus, we can conclude that the hydrogen in the studied MXene $Ti_3C_2T_x$ occupies small cavities. In a situation where hydrogen is bound to the substrate, the drop in intensity on raising the temperature results from a desorption of adsorbed hydrogen [39]. The hydrogen does not disappear from the studied MXene at these temperatures because the sample was annealed at 110 °C in vacuum during the preparation for the INS measurement. The temperature behavior of the peak is also different from the one observed for molecular hydrogen trapped in the interstitial crystallographic positions in C_{60} fullerenes [42] where the peak was still visible on heating while exceeding 80 K. In $Ti_3C_2T_x$, the absence of the peak at $T >\sim 32$ K means that the hydrogen molecules are more mobile than in C_{60} fullerenes and the Debye-Waller factor strongly suppresses the peak's intensity [39]. Note that, in our spectra, the ratio of the para-ortho-transition peak to the background is about 1 to 1 at $T = 5$ K (and worse at higher temperatures) and the underneath part of the spectrum consists of one-phonon and multiphonon neutron scatterings on translational modes of caged water, which have different Q

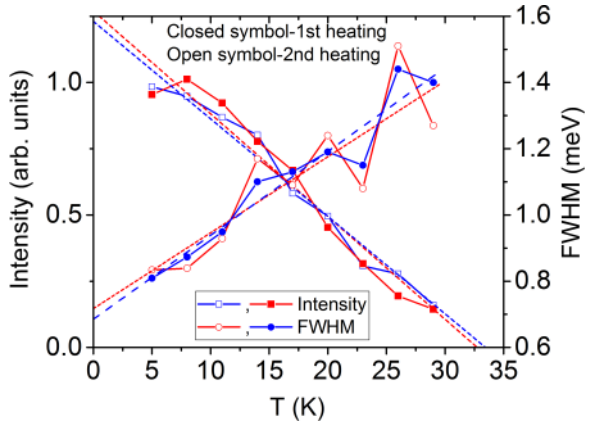

FIG. 3. Temperature dependence of the integrated intensity and the FWHM of the INS peak observed at 14.6 meV from molecular hydrogen trapped in $Ti_3C_2T_x$. The INS spectra were collected at two separate heating scans with an ∼50-h time difference between the scans. The dotted lines are the linear fit of the intensity and the width.

dependences, making it impossible to extract accurately the Q dependence of para- to ortho-H_2 transition peak intensity.

The impact of temperature on the integrated intensity and the width of the peak at 14.6 meV is presented in Fig. 3. Similar to other molecular hydrogen confining media, such as carbon nanohorns [21] and a single walled carbon nanotube [20], we found a decrease in intensity with a subsequent increase in peak broadening (obtained from a Gaussian plus sloped linear background function fit of the peaks) with increasing temperature. This temperature dependence of the peak width should be attributed not to melting but to an increase in mobility (on a time scale of ca. picoseconds, corresponding to the broadening on ca. the meV-energy scale) of the hydrogen molecules due to a decreased interaction with temperature increase, possibly because of a weak van der Waals force between the trapped hydrogen molecules and the $Ti_3C_2T_x$ surface. We observed similar linear temperature dependences of the intensity decrease and the broadening of the peak in two heating scans, thus confirming that the effect is reproducible.

It is interesting to note that the para-ortho-transition peaks in the INS spectrum [Fig. 4(a)] are absent for $Ti_3C_2T_x$-H synthesized using 10% HF and K-intercalated MXene $Ti_3C_2T_x$-K (48% HF), which suggests that a milder concentration of etchant or metal-ion intercalation remove the trapped molecular hydrogen from $Ti_3C_2T_x$. Furthermore, the peaks also were absent in the spectra for $Ti_3C_2T_x$ (48% HF) annealed at 150 °C in vacuum [Fig. 4(b)], revealing that the high temperatures opened the pores confining the molecular hydrogen.

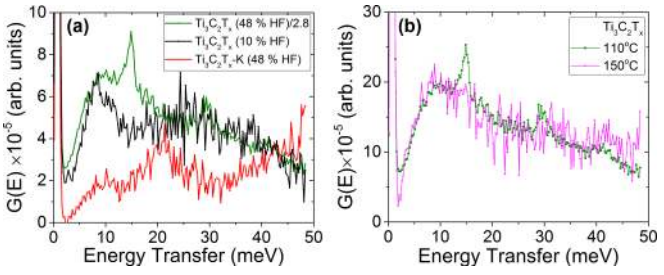

FIG. 4. GVDOS spectra of MXenes measured at $T = 5$ K. (a) A comparison of the spectra collected from pristine and K^+-intercalated MXenes, both annealed at 110 °C in vacuum. The intensity of the spectrum from pristine MXene is decreased by 2.8 times compared to that from K-intercalated MXene. (b) Spectra collected from pristine MXenes annealed at two different temperatures (the intensity for the sample annealed at 150 °C is increased by 2.8 times).

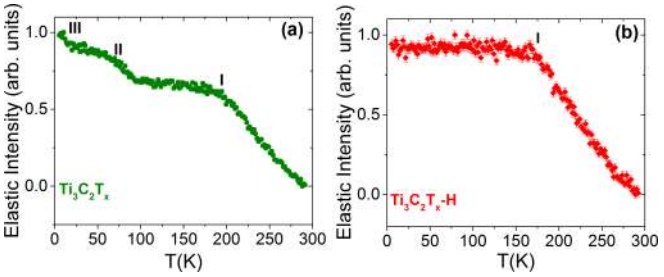

FIG. 5. Elastic neutron-scattering spectra measured at the HFBS spectrometer for different MXene samples: (a) MXene synthesized using 48% of HF, (b) $Ti_3C_2T_x$-H is a MXene synthesized using 10% HF + LiCl that contains H^+ ions between layers. All samples were annealed at 110 °C prior to the measurements. Different dynamic regions are indicated by I, II, and III.

Intensity of the elastic scattering from two MXene samples, synthesized using different procedures, as a function of temperature is presented in Fig. 5. Note that a sudden decrease in the elastic-scattering intensity indicates a change in the behavior of hydrogen-bearing species in the samples. Here, both spectra show a rapid drop (represented as region I) in the elastic intensity above ∼180 K. This decrease in intensity as observed previously in MXenes [24] and other confining media, such as clay [45], is attributed to the presence of confined water that shows increased mobility in this temperature range. It has been reported that all the pristine and ion-intercalated MXenes retain significant amounts of water even after annealing at 110 °C in vacuum.

Elastic intensity spectra of MXene synthesized using 10% HF + LiCl and those intercalated with metal ions (data not shown) remain almost flat [look similar to Fig. 5(b)] between 5 and 180 K, indicating the absence of any hydrogen-bearing species that show mobility in this temperature range. However, the spectrum collected from $Ti_3C_2T_x$ shows two more additional intensity drops (marked as II and III) in the temperature range of 5–180 K. Note that a drop in elastic intensity starting at 60 K has been reported for hydrogen adsorbed in potassium-intercalated graphite $KC_{24}(H_2)_2$ [46]. Here, INS spectra measured from $Ti_3C_2T_x$ did not show any peaks originating from para- to orthotransition at temperatures above 35 K. This means that the mobility of the hydrogen molecules confined in $Ti_3C_2T_x$ becomes so high that it moves beyond the detection limit of the spectrometer. Therefore, we conclude that the drop in elastic intensity at 80 K (region II) is not from the mobility of the hydrogen molecules but from some other hydrogen-bearing species, possibly some form of ultraconfined water [47]. The spectrum of $Ti_3C_2T_x$ displays yet another intensity drop at temperatures of ∼10–35 K as represented by region III. This is the temperature range at which INS reveals the existence of molecular hydrogen in

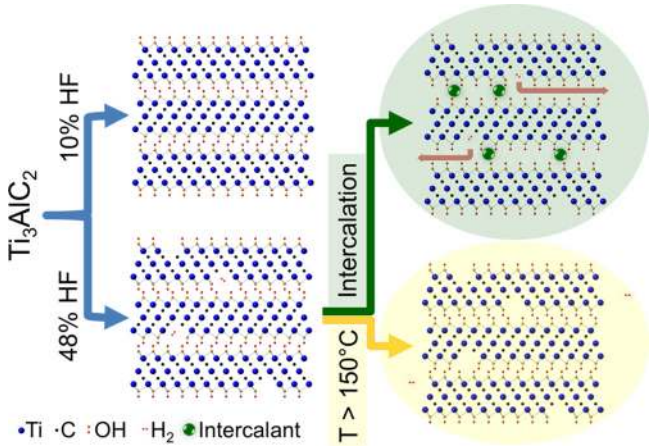

FIG. 6. Schematic showing the processes that result in MXene with and without trapped molecular hydrogen.

$Ti_3C_2T_x$.Therefore, this transition observed in the elastic scan is due to the hydrogen molecules' diffusion. This observation further evidences the presence of molecular hydrogen in $Ti_3C_2T_x$, synthesized using 48% HF solution. It is worth noting here that the elastic intensity presented in Fig. 5 is not noticeably affected by a possible para-ortho-transition of the hydrogen with the temperature change because of the much smaller measurement time compared to characteristic para-ortho-conversion time.

Since we did not get any evidence of trapped hydrogen in other MXene samples synthesized differently (by using less than 10% HF), it is likely that the use of a strong etchant during the etching of the MAX phase creates some voids in the MXene where the hydrogen produced during the etching process becomes trapped. Note that structure studies of MXenes have revealed the presence of defects, such as vacancies and vacancy clusters, in MXene layers [7,48]. The voids that hold molecular hydrogen in $Ti_3C_2T_x$ can be attributed to the defect-induced morphological changes in MXene. The use of a milder etchant (10% HF), ion intercalation, or an increase in annealing temperature yields a less defective structure deprived of hydrogen as illustrated in the schematic shown in Fig. 6.

IV. CONCLUSIONS

Using inelastic and elastic neutron scatterings, we presented the evidence of molecular hydrogen trapped in $Ti_3C_2T_x$ MXene synthesized using 48% HF solution and annealed at 110 °C in vacuum. A peak at 14.6 meV in the INS spectrum of the MXene measured at 5 K confirms the presence of molecular hydrogen. A decrease in the peak intensity and a corresponding peak broadening with a rise in temperature up to 35 K, characteristic of the behavior of confined hydrogen molecules, was observed. The decay of the elastic intensity between 10 and 35 K illustrates the diffusion of the confined hydrogen molecules in $Ti_3C_2T_x$. We did not find molecular hydrogen trapped in other samples, indicating that the change in synthesis procedure, metal-ion intercalation, and/or an increase in annealing temperature removes the trapped hydrogen molecules from MXene. Even though the 0.3-wt % hydrogen content determined in the current paper was obtained naturally in the course of sample synthesis, not intentionally loaded, this experimental finding is in line with the theoretical study [17] that has revealed the potential of MXene for hydrogen storage applications at ambient conditions.

ACKNOWLEDGMENTS

This work was supported as part of the Fluid Interface Reactions, Structures and Transport Center, an Energy Frontier Research Center funded by the U.S. Department of Energy, Office of Science, Office of Basic Energy Sciences. This research used resources at the Spallation Neutron Source, a DOE Office of Science User Facility operated by the Oak Ridge National Laboratory. Experiments on HFBS at the NIST Center for Neutron Research were supported, in part, by the National Science Foundation under Grant Agreement No. DMR-1508249.

[1] M. Naguib, M. Kurtoglu, V. Presser, J. Lu, J. Niu, M. Heon, L. Hultman, Y. Gogotsi, and M. W. Barsoum, Adv. Mater. **23**, 4248 (2011).
[2] B. Anasori, M. Lukatskaya, and Y. Gogotsi, Nat. Rev. Mater. **2**, 16098 (2017).
[3] Y. Xie, M. Naguib, V. N. Mochalin, M. W. Barsoum, Y. Gogotsi, X. Yu, K.-W. Nam, X.-Q. Yang, A. I. Kolesnikov, and P. R. C. Kent, J. Am. Chem. Soc. **136**, 6385 (2014).
[4] Y. Jing, Z. Zhou, C. R. Cabrera, and Z. F. Chen, J. Mater. Chem. A **2**, 12104 (2014).
[5] K. Hantanasirisakul, M. Q. Zhao, P. Urbankowski, J. Halim, B. Anasori, S. Kota, C. E. Ren, M. W. Barsoum, and Y. Gogotsi, Adv. Electron. Mater. **2**, 1600050 (2016).
[6] M. Naguib and Y. Gogotsi, Acc. Chem. Res. **48**, 128 (2015).
[7] H. W. Wang, M. Naguib, K. Page, D. J. Wesolowski, and Y. Gogotsi, Chem. Mater. **28**, 349 (2016).
[8] M. A. Hope, A. C. Forse, K. J. Griffith, M. R. Lukatskaya, M. Ghidiu, Y. Gogotsi, and C. P. Grey, Phys. Chem. Chem. Phys. **18**, 5099 (2016).
[9] O. Mashtalir, M. Naguib, V. N. Mochalin, Y. Dall'Agnese, M. Heon, M. W. Barsoum, and Y. Gogotsi, Nat. Commun. **4**, 1716 (2013).
[10] M. R. Lukatskaya, O. Mashtalir, C. E. Ren, Y. Dall'Agnese, P. Rozier, P. L. Taberna, M. Naguib, P. Simon, M. W. Barsoum, and Y. Gogotsi, Science **341**, 1502 (2013).
[11] C. Eames, and M. S. Islam, J. Am. Chem. Soc. **136**, 16270 (2014).
[12] N. M. Musyoka and H. W. Langmi, *Clay and Clay-Supported Materials for Clean Energy Storage Applications* (Nova Science, New York, 2015).
[13] F. Campos, L. de la Torre, M. Roman, A. Garcia, and A. A. Elguezabal, J. Ceram. Process. Res. **9**, 482 (2008).

[14] A. Szucs, Z. Kiraly, F. Berger, and I. Dekany, Colloids Surf., A **139**, 109 (1998).
[15] X. F. Wang, X. Shen, Y. R. Gao, Z. X. Wang, R. C. Yu, and L. Q. Chen, J. Am. Chem. Soc. **137**, 2715 (2015).
[16] O. Mashtalir, M. R. Lukatskaya, A. I. Kolesnikov, E. Raymundo-Pinero, M. Naguib, M. W. Barsoum, and Y. Gogotsi, Nanoscale **8**, 9128 (2016).
[17] Q. K. Hu, D. D. Sun, Q. H. Wu, H. Y. Wang, L. B. Wang, B. Z. Liu, A. G. Zhou, and J. L. He, J. Phys. Chem. A **117**, 14253 (2013).
[18] Z. W. Seh, K. D. Fredrickson, B. Anasori, J. Kibsgaard, A. L. Strickler, M. R. Lukatskaya, Y. Gogotsi, T. F. Jaramillo, and A. Vojvodic, ACS Energy Lett. **1**, 589 (2016).
[19] M. R. Lukatskaya, S. M. Bak, X. Q. Yu, X. Q. Yang, M. W. Barsoum, and Y. Gogotsi, Adv. Energy Mater. **5**, 1500589 (2015).
[20] Y. Ren and D. L. Price, Appl. Phys. Lett. **79**, 3684 (2001).
[21] F. Fernandez-Alonso, F. J. Bermejo, C. Cabrillo, R. O. Loutfy, V. Leon, and M. L. Saboungi, Phys. Rev. Lett. **98**, 215503 (2007).
[22] L. Smrcok, D. Tunega, A. J. Ramirez-Cuesta, A. Ivanov, and J. Valuchova, Clays Clay Miner. **58**, 52 (2010).
[23] N. C. Osti, A. Cote, E. Mamontov, A. Ramirez-Cuesta, D. J. Wesolowski, and S. O. Diallo, Chem. Phys. **465-466**, 1 (2016).
[24] N. C. Osti, M. Naguib, A. Ostadhossein, Y. Xie, P. R. C. Kent, B. Dyatkin, G. Rother, W. T. Heller, A. C. T. van Duin, Y. Gogotsi, and E. Mamontov, ACS Appl. Mater. Interfaces **8**, 8859 (2016).
[25] A. I. Kolesnikov, G. F. Reiter, N. Choudhury, T. R. Prisk, E. Mamontov, A. Podlesnyak, G. Ehlers, A. G. Seel, D. J. Wesolowski, and L. M. Anovitz, Phys. Rev. Lett. **116**, 167802 (2016).
[26] M. Ghidiu, J. Halim, S. Kota, D. Bish, Y. Gogotsi, and M. W. Barsourm, Chem. Mater. **28**, 3507 (2016).
[27] G. E. Granroth, A. I. Kolesnikov, T. E. Sherline, J. P. Clancy, K. A. Ross, J. P. C. Ruff, B. D. Gaulin, S. E. Nagler, J. Phys.: Conf. Ser. **251**, 012058 (2010).
[28] M. B. Stone, J. L. Niedziela, D. L. Abernathy, L. DeBeer-Schmitt, G. Ehlers, O. Garlea, G. E. Granroth, M. Graves-Brook, A. I. Kolesnikov, A. Podlesnyak, and B. Winn, Rev. Sci. Instrum. **85**, 045113 (2014).
[29] O. Arnold, J. C. Bilheux, J. M. Borreguero, A. Buts, S. I. Campbell, L. Chapon, M. Doucet, N. Draper, R. F. Leal, M. A. Gigg, V. E. Lynch, A. Markyardsen, D. J. Mikkelson, R. L. Mikkelson, R. Miller, K. Palmen, P. Parker, G. Passos, T. G. Perring, P. F. Peterson, S. Ren, M. A. Reuter, A. T. Sayici, J. W. Taylor, R. J. Taylor, R. Tolchenoy, W. Zhou, and J. Zikoysky, Nucl. Instrum. Methods Phys. Res., Sect. A **764**, 156 (2014).
[30] R. T. Azuah, L. R. Kneller, Y. M. Qiu, P. L. W. Tregenna-Piggott, C. M. Brown, J. R. D. Copley, and R. M. Dimeo, J. Res. Natl. Inst. Stand. Technol. **114**, 341 (2009).
[31] A. Meyer, R. Dimeo, P. Gehring, and D. Neumann, Rev. Sci. Instrum. **74**, 2759 (2003).
[32] C. L. Thaper, B. A. Dasannacharya, A. Sequeira, and P. K. Iyengar, Solid State Commun. **8**, 497 (1970).
[33] C. M. B. Line and G. J. Kearley, J. Chem. Phys. **112**, 9058 (2000).
[34] J. C. Li and A. I. Kolesnikov, J. Mol. Liq. **100**, 1 (2002).
[35] H. W. Wang, M. J. DelloStritto, N. Kumar, A. I. Kolesnikov, P. R. C. Kent, J. D. Kubicki, D. J. Wesolowski, and J. O. Sofo, J. Phys. Chem. C **118**, 10805 (2014).
[36] J. C. Li, J. Chem. Phys. **105**, 6733 (1996).
[37] I. F. Silvera, Rev. Mod. Phys. **52**, 393 (1980).
[38] L. Senadheera, E. M. Carl, T. M. Ivancic, M. S. Conradi, R. C. Bowman, S. J. Hwang, and T. J. Udovic, J. Alloys Compd. **463**, 1 (2008).
[39] S. F. Parker, C. D. Frost, M. Telling, P. Albers, M. Lopez, and K. Seitz, Catal. Today **114**, 418 (2006).
[40] K. Fukutani and T. Sugimoto, Prog. Surf. Sci. **88**, 279 (2013).
[41] P. A. Georgiev, D. K. Ross, P. Albers, and A. J. Ramirez-Cuesta, Carbon **44**, 2724 (2006).
[42] S. A. FitzGerald, T. Yildirim, L. J. Santodonato, D. A. Neumann, J. R. D. Copley, J. J. Rush, and F. Trouw, Phys. Rev. B **60**, 6439 (1999).
[43] M. Nielsen, J. P. McTague, and W. Ellenson, J. Phys., Colloq. **38**, C4-10 (1977).
[44] M. Celli, D. Colognesi, and M. Zoppi, Phys. Rev. E **66**, 021202 (2002).
[45] H. N. Bordallo, L. P. Aldridge, G. J. Churchman, W. P. Gates, M. T. F. Telling, K. Kiefer, P. Fouquet, T. Seydel, and S. A. J. Kimber, J. Phys. Chem. C **112**, 13982 (2008).
[46] J. J. Purewal, J. B. Keith, C. C. Ahn, B. Fultz, C. M. Brown, and M. Tyagi, Phys. Rev. B **79**, 054305 (2009).
[47] A. I. Kolesnikov, L. M. Anovitz, E. Mamontov, A. Podlesnyak, and G. Ehlers, J. Phys. Chem. B **118**, 13414 (2014).
[48] X. H. Sang, Y. Xie, M. W. Lin, M. Alhabeb, K. L. Van Aken, Y. Gogotsi, P. R. C. Kent, K. Xiao, and R. R. Unocic, ACS Nano **10**, 9193 (2016).